HHS Public Access

Author manuscript

J Am Chem Soc. Author manuscript; available in PMC 2022 July 25.

Published in final edited form as:

J Am Chem Soc. 2021 April 21; 143(15): 5674–5679. doi:10.1021/jacs.1c02112.

Norcyanine-Carbamates Are Versatile Near-Infrared Fluorogenic Probes

Syed Muhammad Usama,
Chemical Biology Laboratory, Center for Cancer Research, National Cancer Institute, Frederick, Maryland 21702, United States

Fuyuki Inagaki,
Molecular Imaging Branch, Center for Cancer Research, National Cancer Institute, National Institutes of Health, Bethesda, Maryland 20892, United States

Hisataka Kobayashi,
Molecular Imaging Branch, Center for Cancer Research, National Cancer Institute, National Institutes of Health, Bethesda, Maryland 20892, United States

Martin J. Schnermann
Chemical Biology Laboratory, Center for Cancer Research, National Cancer Institute, Frederick, Maryland 21702, United States

Abstract

Fluorogenic probes in the near-infrared (NIR) region have the potential to provide stimuli-dependent information in living organisms. Here, we describe a new class of fluorogenic probes based on the heptamethine cyanine scaffold, the most broadly used NIR chromophore. These compounds result from modification of heptamethine norcyanines with stimuli-responsive carbamate linkers. The resulting cyanine carbamates (CyBams) exhibit exceptional turn-ON ratios (~170×) due to dual requirements for NIR emission: carbamate cleavage through 1,6-elimination and chromophore protonation. Illustrating their utility in complex *in vivo* settings, a γ-glutamate substituted CyBam was applied to imaging γ-glutamyl transpeptidase (GGT) activity in a metastatic model of ovarian cancer. Overall, CyBams have significant potential to extend the reach of fluorogenic strategies to intact tissue and live animal imaging applications.

Selectively activating a fluorescent signal is a powerful approach to interrogate biological processes. A common tactic uses multichromophore systems that rely on quenching through fluorescence resonance energy transfer (FRET) and related mechanisms.[1] Another approach

Corresponding Author Martin J. Schnermann – martin.schnermann@nih.gov.

The authors declare the following competing financial interest(s): S.M.U. and M.J.S. have applied for a patent based on this work.

Complete contact information is available at: https://pubs.acs.org/10.1021/jacs.1c02112

Supporting Information

The Supporting Information is available free of charge at https://pubs.acs.org/doi/10.1021/jacs.1c02112.

Synthetic details and characterization of **CyBam-N$_3$, CyBam-γ-Glu, CyBam-N.C., CyBam-B(OH)$_2$, CyBam-P(OPh)$_2$,** and their intermediates; supplementary figures; detailed information on enzymatic, *in vitro*, and *in vivo* assays; additional data and figures including absorbance and fluorescence spectra, photophysical properties, Staudinger release, stability values, pK_a values, pH values, rate of activation, kinetics of fluorogenic probe activation, inhibition quantification, toxicity data, cellular uptake, confocal imaging, flow cytometry analyses, and bright-field imaging (PDF)

uses fluorogenic probes, where the change in signal results from chemical transformations to the chromophore itself.[2–6] The latter often provides improved turn-ON ratios and benefits from requiring only a single chromophore. The most broadly used fluorogenic chemistry is based on derivatization of coumarin, rhodamine, and hybrid cyanine scaffolds, which absorb and emit light in the visible to far-red range.[4,5,7–10] To carry out such experiments in living organisms, it is desirable to have turn-ON probes that absorb and emit long-wavelength near-infrared (NIR) light (>700 nm), which is less attenuated by tissue. However, only systems based on FRET pairs or self-quenching have routinely been applied in this range (Figure 1A).[11–14]

Indocyanine dyes are exceptionally useful fluorescent probes. Heptamethine cyanines such as indocyanine green (ICG) and IR-800CW have been the subject of extensive preclinical and clinical *in vivo* imaging efforts.[15,16] Fluorogenic probes built on the heptamethine cyanine scaffold would benefit from the extensive infrastructure built for their use, as well as previous efforts to optimize these molecules.[13,14] We hypothesized that such probes could be created by carbamate derivatization of norcyanines; a class of molecules originally reported by Miltsov characterized by secondary, not tertiary, indolenine nitrogen atoms attached to the polymethine chromophore.[17–19] These dyes differ from conventional cyanines in that their NIR fluorescent signal requires nitrogen protonation (pK_a ~ 5). Achilefu and co-workers have demonstrated the exceptional utility of water-soluble variants of these dyes for *in vivo* tumor imaging.[20,21]

Here, we report the synthesis, validation, and application of a series of fluorogenic cyanine carbamates, or CyBams, that can be activated by a range of stimuli (Figure 1B). We demonstrate that sulfonated heptamethine norcyanines can be derivatized with a range of cleavable benzyl carbamates to provide the stable CyBam probes (λ_{abs} = 430 nm). These molecules then undergo efficient triggered 1,6-elimination to provide the pH-responsive heptamethine norcyanines (protonated form λ_{abs} = 755 nm). Unlike existing far-red fluorogenic probes, the cationic chromophore is only formed through carbamate cleavage and nitrogen protonation, leading to an exceptional turn-ON ratio (>150×). A glutamate substituted CyBam can be activated by γ-glutamyl transpeptidase (GGT) with high selectivity *in vitro* and in a metastatic model of ovarian cancer. Overall, these studies provide a new class of versatile NIR fluorogenic probes with significant potential to extend turn-ON strategies to *in vivo* applications.

To test this approach, we first prepared a disulfonated heptamethine norcyanine, **NorCy7**, a decarboxylated form of a compound previously reported by Achilefu.[21] In line with prior reports, the dye exhibits two forms in biologically relevant conditions, an unprotonated quenched form, **NorCy7** (λ_{abs} = 520 nm @ pH 7.4), and a protonated fluorescent form, **NorCy7-[H$^+$]** (λ_{abs} = 755 nm @ pH 4.5), with a pK_a of 5.2 (Figure S1a,b). After examining several conditions, we were delighted to find that exposure of **NorCy7** and 4-nitrophenyl carbonates to NaH or Cs_2CO_3 in DMF afforded the corresponding carbamate products. Using this approach, we prepared **CyBam-N$_3$** from **NorCy7** and **1** in reasonable yield following purification by reversed-phase chromatography (Scheme 1).

CyBam-N_3 allowed us to examine the turn-ON chemistry using a chemical trigger. Azide reduction, involving aza-ylide formation and hydrolysis, was hypothesized to initiate 1,6-elimination and carbamic acid hydrolysis to result in unmasking of the pH-sensitive norcyanine (Figure 2A).[22–24] **CyBam-N_3** exhibits minimal absorbance and emission in the NIR range at either neutral (pH 7.2) or acidic (pH 4.5) conditions (Figure 2B, Figure S2). As anticipated, examining the absorbance profile of **CyBam-N_3** and **NorCy7** at both neutral and acidic pH revealed three readily distinguishable species (Figure 2B,C). We investigated the stability of **CyBam-N_3** at physiological pHs and in serum and observed little degradation (<5%) over 24 h (Figure S4). Next, we examined the fluorogenic response of **CyBam-N_3** by incubating with PPh_3 at pH 5.2 (Figure 2D). We observed rapid conversion to **NorCy7-[H^+]** with a dramatic 170-fold increase in the fluorescence signal (Figure 2E). This reaction could also be carried out at neutral pH to provide the neutral form **NorCy7** (Figure S3). Lastly, we compared the magnitude of the turn-ON response of CyBams to xanthene cyanines, which are far-red probes that have been broadly employed for *in vivo* fluorogenic imaging.[10,25–28] We prepared and tested a sulfonated, acetylated variant and found turn-ON ratios of 1.5 and 15 (with 640 nm ex.) at pH 4.5 and 7.2, respectively (Figure S5). The critical distinction is the absorption profile in the OFF state. The acetylated xanthene cyanines exhibit a substantial long-wavelength absorption band, which leads to significant emission from the quenched state (Figure S5). By contrast, CyBams exhibit minimal absorption in the NIR region at either neutral or acidic pHs.

To investigate the utility of CyBams for cellular and *in vivo* imaging, we used a validated fluorogenic trigger with significant translational potential. GGT is a cell-surface-bound enzyme involved in maintaining cellular glutathione (GSH) and cysteine homeostasis.[29–32] Additionally, it has been used as a biomarker of several malignant tumors (including liver, cervical, and ovarian), and overexpression of GGT has been correlated with metastases.[33–36] The key cleavable glutamate was installed on **CyBam-γ-Glu** (Figure 3A) using a similar procedure to that described above (see the Supporting Information). After confirming the stability of **CyBam-γ-Glu** (Figure S6), we examined the probe in enzymatic assays. We observed a GGT-dependent increase in fluorescent signal (Figure 3B) with a Michaelis constant (K_M =16 μM) similar to those obtained with other GGT probes (Figure S7).[37] We also established that **CyBam-γ-Glu** is specifically activated by GGT and did not show any significant signal when incubated with representative proteases and esterases (Figure 3C). Lastly, we determined the selectivity of **CyBam-γ-Glu** using established GGT inhibitors.[38,39] We observed a 60% and 80% decrease in fluorescent signal in the presence of DON and GGsTop, respectively, confirming the selectivity of the probe (Figure S8).

We then examined **CyBam-γ-Glu**, and the corresponding noncleavable variant **CyBam-N.C.,** in cellular assays and *in vivo* imaging experiments (Figure 3A). We used a SHIN-3 ovarian cancer cell line that has been previously shown to overexpress GGT.[40] We first established that **CyBam-γ-Glu** exhibited minimal toxicity (Figure S9). We also established that **NorCy7** exhibited significant cellular uptake in SHIN-3 cells. The majority of the fluorescent signal was observed in lysosomes, where the acidic microenvironment is likely responsible for formation of **NorCy7-[H^+]** (Figure S10).[21] Next, we evaluated the cellular activation and selectivity of **CyBam-γ-Glu** with and without incubation with

GGT inhibitors. Using confocal microscopy and flow cytometry, we observed a strong fluorescent signal in cells treated with **CyBam-γ-Glu.** By contrast, minimal fluorescence signal was observed in cells that were either treated with **CyBam-N.C.** or preincubated with GGT inhibitors (Figure 3D,E and Figures S11 and S12). Encouraged by these results, we tested **CyBam-γ-Glu** in a metastatic tumor model of ovarian cancer. This model entails intraperitoneal injection of SHIN-3-ZsGreen cells, resulting in formation of a significant primary tumor in the greater omentum and locally disseminated metastases.[40] **CyBam-γ-Glu** (30 nmol) was injected intraperitoneally in mice, which were euthanized after 1, 3, and 6 h, and both the primary tumor and local metastases were imaged. Excellent colocalization between **CyBam-γ-Glu** and the ZsGreen signal suggests that the probe was activated and taken up selectively by tumor cells, with a significant signal at all three time points (Figure 3F and Figures S13 and S14). We also confirmed that these probes can be used in live mice using a conventional *in vivo* imaging system (IVIS). To do this, we compared **CyBam-γ-Glu** and **CyBam-N.C.** in an MDA-MB-468 xenograft, which is a triple-negative breast cancer cell line with modest GGT expression.[41,42] The **CyBam-γ-Glu** can be readily visualized with significant differences between the two agents in both tumor and liver signals, as well as tumor-to-background ratios (Figure S15).

Finally, to examine the versatility of this approach, we prepared and initially characterized the utility of CyBam probes to visualize common reactive oxygen species (ROS) with well-validated ROS-responsive triggers: boronic acid (H_2O_2) and phosphine oxide (O_2^{-}).[7,43,44] We tested the induction of ROS in PC-3 cells, a prostate cancer cell line, by doxorubicin. Notably, doxorubicin absorbs in the visible region (λ_{max} = 480 nm) which can hamper the utility of conventional visible light-absorbing fluorogenic probes.[45,46] As expected, we observed the generation of both superoxide and hydrogen peroxide, with no interference from the addition of doxorubicin (Figures S16 and S17). These results suggest that these probes may have significant utility in the exploration of ROS biology.

Fluorogenic probes are powerful tools with the potential to noninvasively monitor enzymatic processes and other stimuli in real-time in living organisms. Here, we report CyBams, the first enzyme- or analyte-responsive fluorogenic probes based on the heptamethine cyanine scaffold. These readily water-soluble probes result from modification of the norcyanine scaffold with a cleavable carbamate linker that is activated through 1,6-elimination and chromophore protonation. This combination results in turn-ON ratios that dramatically exceed those found with existing far-red fluorogenic probes, particularly in acidic conditions. The results presented above suggest that CyBams have significant potential for use as activatable probes for *in vivo* imaging. We hypothesize their application may include optically guided surgical procedures and note that the extensive optical instrumentation in place for heptamethine cyanines makes this prospect more enticing.[47] Going forward, as CyBams are more emissive upon protonation in the lysosome, it is possible that efforts to improve their lysosomal targeting may serve to increase their signal intensity. Additionally, as cyanine fluorophores have historically been most useful as bioconjugatable probes, we anticipate that the utility of CyBams may be enhanced when combined with active targeting. In this scenario, targetable CyBams create the possibility to report on enzymatic activity at

only a specific cell type or location of interest. Efforts toward these goals are ongoing and will be reported in due course.

Supplementary Material

Refer to Web version on PubMed Central for supplementary material.

ACKNOWLEDGMENTS

This work was supported by the Intramural Research Program of the National Institutes of Health (NIH), NCI-CCR. We acknowledge Dr. James A. Kelley (National Cancer Institute) for providing the high-resolution mass spectrometry analysis. We thank Dr. Gary T. Pauly (National Cancer Institute) for assisting with LC/MS and HPLC purification. We would also like to thank Dr. Valentin Magidson, NCI-Optical Microscopy laboratory, and Dr. Jeff Carrell (CCR-Frederick Flow Cytometry Core Laboratory) for assisting with confocal microscopy and flow cytometry, respectively. Finally, we thank Nimit L. Patel, Lisa Riffle and Joseph D. Kalen (Small Animal Imaging Program), and Chelsea Sanders and Simone Difilippantonio (Laboratory Animal Sciences Program) for assistance with the *in vivo* study.

ABBREVIATIONS

NIR	near-infrared
FRET	fluorescence resonance energy transfer
CyBam	cyanine carbamate
ICG	indocyanine green
LAP	leucine aminopeptidase
PLE	pig-liver esterase
CatB	cathepsin B
PBS	phosphate buffer saline
GGT	γ-glutamyl transpeptidase
γ-Glu	γ-glutamate
DON	6-diazo-5-oxo-L-norleucine
GGsTop	2-amino-4[3-(carboxymethyl)-phenyl](methyl)phosphono-butanoic acid
GSH	glutathione
GFP	green fluorescent protein
Cy7	heptamethine
DMF	dimethylformamide
NaH	sodium hydride
Cs_2CO_3	cesium carbonate

abs	absorbance
ex	excitation
em	emission
N.A.	numerical aperture

REFERENCES

(1). Wu L; Huang C; Emery BP; Sedgwick AC; Bull SD; He XP; Tian H; Yoon J; Sessler JL; James TD Forster resonance energy transfer (FRET)-based small-molecule sensors and imaging agents. Chem. Soc. Rev 2020, 49 (15), 5110–5139. [PubMed: 32697225]

(2). Kobayashi H; Ogawa M; Alford R; Choyke PL; Urano Y New strategies for fluorescent probe design in medical diagnostic imaging. Chem. Rev 2010, 110 (5), 2620–40. [PubMed: 20000749]

(3). Grimm JB; Heckman LM; Lavis LD The Chemistry of Small-Molecule Fluorogenic Probes. Prog. Mol. Biol. Transl 2013, 113, 1–34.

(4). Chyan W; Raines RT Enzyme-Activated Fluorogenic Probes for Live-Cell and in Vivo Imaging. ACS Chem. Biol 2018, 13 (7), 1810–1823. [PubMed: 29924581]

(5). Jun JV; Chenoweth DM; Petersson EJ Rational design of small molecule fluorescent probes for biological applications. Org. Biomol. Chem 2020, 18 (30), 5747–5763. [PubMed: 32691820]

(6). Shieh P; Hangauer MJ; Bertozzi CR Fluorogenic azidofluoresceins for biological imaging. J. Am. Chem. Soc 2012, 134 (42), 17428–31. [PubMed: 23025473]

(7). Chan J; Dodani SC; Chang CJ Reaction-based small-molecule fluorescent probes for chemoselective bioimaging. Nat. Chem 2012, 4 (12), 973–84. [PubMed: 23174976]

(8). Zhang J; Chai X; He XP; Kim HJ; Yoon J; Tian H Fluorogenic probes for disease-relevant enzymes. Chem. Soc. Rev 2019, 48 (2), 683–722. [PubMed: 30520895]

(9). Karton-Lifshin N; Albertazzi L; Bendikov M; Baran PS; Shabat D "Donor-two-acceptor" dye design: a distinct gateway to NIR fluorescence. J. Am. Chem. Soc 2012, 134 (50), 20412–20. [PubMed: 23194283]

(10). Yuan L; Lin W; Zhao S; Gao W; Chen B; He L; Zhu S A unique approach to development of near-infrared fluorescent sensors for in vivo imaging. J. Am. Chem. Soc 2012, 134 (32), 13510–23. [PubMed: 22816866]

(11). Widen JC; Tholen M; Yim JJ; Antaris A; Casey KM; Rogalla S; Klaassen A; Sorger J; Bogyo M AND-gate contrast agents for enhanced fluorescence-guided surgery. Nat. Biomed Eng 2021, 5, 264. [PubMed: 32989286]

(12). Ofori LO; Withana NP; Prestwood TR; Verdoes M; Brady JJ; Winslow MM; Sorger J; Bogyo M Design of Protease Activated Optical Contrast Agents That Exploit a Latent Lysosomotropic Effect for Use in Fluorescence-Guided Surgery. ACS Chem. Biol 2015, 10, 1977. [PubMed: 26039341]

(13). Chen C; Tian R; Zeng Y; Chu C; Liu G Activatable Fluorescence Probes for "Turn-On" and Ratiometric Biosensing and Bioimaging: From NIR-I to NIR-II. Bioconjugate Chem 2020, 31 (2), 276–292.

(14). Gorka AP; Nani RR; Schnermann MJ Cyanine polyene reactivity: scope and biomedical applications. Org. Biomol. Chem 2015, 13 (28), 7584–98. [PubMed: 26052876]

(15). Gorka AP; Nani RR; Schnermann MJ Harnessing Cyanine Reactivity for Optical Imaging and Drug Delivery. Acc. Chem. Res 2018, 51 (12), 3226–3235. [PubMed: 30418020]

(16). Usama SM; Thapaliya ER; Luciano MP; Schnermann MJ Not so innocent: Impact of fluorophore chemistry on the in vivo properties of bioconjugates. Curr. Opin. Chem. Biol 2021, 63, 38–45. [PubMed: 33684856]

(17). Miltsov S; Encinas C; Alonso JN Nortricarbocyanines: New near-infrared pH-indicators. Tetrahedron Lett 1998, 39 (50), 9253–9254.

(18). Briggs MS; Burns DD; Cooper ME; Gregory SJ A pH sensitive fluorescent cyanine dye for biological applications. Chem. Commun 2000, No. 23, 2323–2324.

(19). Zhang Z; Achilefu S Design, synthesis and evaluation of near-infrared fluorescent pH indicators in a physiologically relevant range. Chem. Commun 2005, No. 47, 5887–9.

(20). Lee H; Akers W; Bhushan K; Bloch S; Sudlow G; Tang R; Achilefu S Near-infrared pH-activatable fluorescent probes for imaging primary and metastatic breast tumors. Bioconjugate Chem 2011, 22 (4), 777–84.

(21). Gilson RC; Tang R; Som A; Klajer C; Sarder P; Sudlow GP; Akers WJ; Achilefu S Protonation and Trapping of a Small pH-Sensitive Near-Infrared Fluorescent Molecule in the Acidic Tumor Environment Delineate Diverse Tumors in Vivo. Mol. Pharmaceutics 2015, 12 (12), 4237–46.

(22). Lukasak B; Morihiro K; Deiters A Aryl Azides as Phosphine-Activated Switches for Small Molecule Function. Sci. Rep 2019, 9 (1), 1470. [PubMed: 30728367]

(23). Hai Z; Wu J; Wang L; Xu J; Zhang H; Liang G Bioluminescence Sensing of gamma-Glutamyltranspeptidase Activity In Vitro and In Vivo. Anal. Chem 2017, 89 (13), 7017–7021. [PubMed: 28605900]

(24). Wang Y; Li J; Feng L; Yu J; Zhang Y; Ye D; Chen HY Lysosome-Targeting Fluorogenic Probe for Cathepsin B Imaging in Living Cells. Anal. Chem 2016, 88 (24), 12403–12410. [PubMed: 28193055]

(25). Huang J; Lyu Y; Li J; Cheng P; Jiang Y; Pu K A Renal-Clearable Duplex Optical Reporter for Real-Time Imaging of Contrast-Induced Acute Kidney Injury. Angew. Chem., Int. Ed 2019, 58 (49), 17796–17804.

(26). Huang J; Li J; Lyu Y; Miao Q; Pu K Molecular optical imaging probes for early diagnosis of drug-induced acute kidney injury. Nat. Mater 2019, 18 (10), 1133–1143. [PubMed: 31133729]

(27). Cheng P; Chen W; Li S; He S; Miao Q; Pu K Fluoro-Photoacoustic Polymeric Renal Reporter for Real-Time Dual Imaging of Acute Kidney Injury. Adv. Mater 2020, 32 (17), e1908530. [PubMed: 32141674]

(28). Huang J; Jiang Y; Li J; He S; Huang J; Pu K A Renal-Clearable Macromolecular Reporter for Near-Infrared Fluorescence Imaging of Bladder Cancer. Angew. Chem., Int. Ed 2020, 59 (11), 4415–4420.

(29). West MB; Chen Y; Wickham S; Heroux A; Cahill K; Hanigan MH; Mooers BH Novel insights into eukaryotic gamma-glutamyltranspeptidase 1 from the crystal structure of the glutamatebound human enzyme. J. Biol. Chem 2013, 288 (44), 31902–13. [PubMed: 24047895]

(30). Griffith OW; Meister A Translocation of intracellular glutathione to membrane-bound gamma-glutamyl transpeptidase as a discrete step in the gamma-glutamyl cycle: glutathionuria after inhibition of transpeptidase. Proc. Natl. Acad. Sci. U. S. A 1979, 76 (1), 268–72. [PubMed: 34150]

(31). Griffith OW; Bridges RJ; Meister A Evidence that the gamma-glutamyl cycle functions in vivo using intracellular glutathione: effects of amino acids and selective inhibition of enzymes. Proc. Natl. Acad. Sci. U. S. A 1978, 75 (11), 5405–8. [PubMed: 31622]

(32). Wickham S; West MB; Cook PF; Hanigan MH Gamma-glutamyl compounds: substrate specificity of gamma-glutamyl transpeptidase enzymes. Anal. Biochem 2011, 414 (2), 208–14. [PubMed: 21447318]

(33). Schafer C; Fels C; Brucke M; Holzhausen HJ; Bahn H; Wellman M; Visvikis A; Fischer P; Rainov NG Gamma-glutamyl transferase expression in higher-grade astrocytic glioma. Acta Oncol 2001, 40 (4), 529–35. [PubMed: 11504314]

(34). Yao D; Jiang D; Huang Z; Lu J; Tao Q; Yu Z; Meng X Abnormal expression of hepatoma specific gamma-glutamyl transferase and alteration of gamma-glutamyl transferase gene methylation status in patients with hepatocellular carcinoma. Cancer 2000, 88 (4), 761–9. [PubMed: 10679644]

(35). Luo M; Sun W; Wu C; Zhang L; Liu D; Li W; Mei Q; Hu G High pretreatment serum gamma-glutamyl transpeptidase predicts an inferior outcome in nasopharyngeal carcinoma. Oncotarget 2017, 8 (40), 67651–67662. [PubMed: 28978060]

(36). Hanigan MH; Frierson HF Jr.; Brown JE; Lovell MA; Taylor PT Human ovarian tumors express gamma-glutamyl transpeptidase. Cancer Res 1994, 54 (1), 286–290. [PubMed: 7903206]

(37). Li L; Shi W; Wu X; Li X; Ma H In vivo tumor imaging by a gamma-glutamyl transpeptidase-activatable near-infrared fluorescent probe. Anal. Bioanal. Chem 2018, 410 (26), 6771–6777. [PubMed: 29909457]

(38). Han L; Hiratake J; Kamiyama A; Sakata K Design, synthesis, and evaluation of gamma-phosphono diester analogues of glutamate as highly potent inhibitors and active site probes of gamma-glutamyl transpeptidase. Biochemistry 2007, 46 (5), 1432–47. [PubMed: 17260973]

(39). Terzyan SS; Cook PF; Heroux A; Hanigan MH Structure of 6-diazo-5-oxo-norleucine-bound human gamma-glutamyl transpeptidase 1, a novel mechanism of inactivation. Protein Sci 2017, 26 (6), 1196–1205. [PubMed: 28378915]

(40). Urano Y; Sakabe M; Kosaka N; Ogawa M; Mitsunaga M; Asanuma D; Kamiya M; Young MR; Nagano T; Choyke PL; Kobayashi H Rapid cancer detection by topically spraying a gamma-glutamyltranspeptidase-activated fluorescent probe. Sci. Transl. Med 2011, 3 (110), 110ra119.

(41). Pompella A; De Tata V; Paolicchi A; Zunino F Expression of gamma-glutamyltransferase in cancer cells and its significance in drug resistance. Biochem. Pharmacol 2006, 71 (3), 231–8. [PubMed: 16303117]

(42). Dawson J; Smith GD; Boak J; Peters TJ gamma-Glutamyltransferase in human and mouse breast tumours. Clin. Chim. Acta 1979, 96 (1–2), 37–42. [PubMed: 38923]

(43). Xu K; Liu X; Tang B; Yang G; Yang Y; An L Design of a phosphinate-based fluorescent probe for superoxide detection in mouse peritoneal macrophages. Chem. - Eur. J 2007, 13 (5), 1411–6. [PubMed: 17072931]

(44). Chang MC; Pralle A; Isacoff EY; Chang CJ A selective, cell-permeable optical probe for hydrogen peroxide in living cells. J. Am. Chem. Soc 2004, 126 (47), 15392–3. [PubMed: 15563161]

(45). Wagner BA; Evig CB; Reszka KJ; Buettner GR; Burns CP Doxorubicin increases intracellular hydrogen peroxide in PC3 prostate cancer cells. Arch. Biochem. Biophys 2005, 440 (2), 181–90. [PubMed: 16054588]

(46). Wellington KW Understanding cancer and the anticancer activities of naphthoquinones - a review. RSC Adv 2015, 5 (5), 20309–20338.

(47). Barth CW; Gibbs SL Fluorescence Image-Guided Surgery a Perspective on Contrast Agent Development. Proc. SPIE Int. Soc. Opt Eng 2020, 11222, 18.

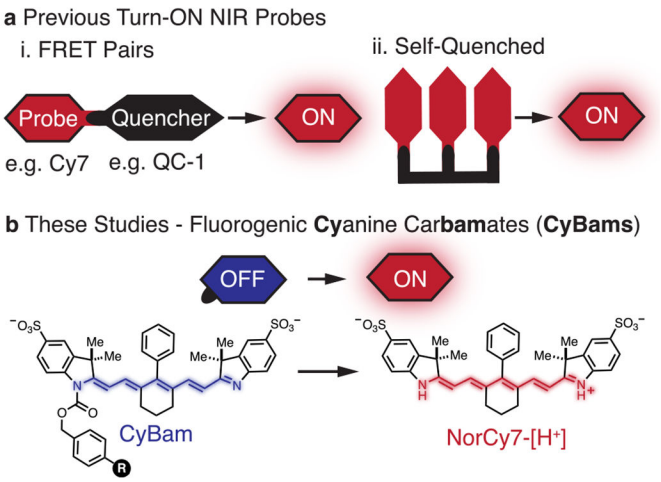

Figure 1.

(a) Previous NIR turn-ON approaches and (b) fluorogenic CyBams reported here.

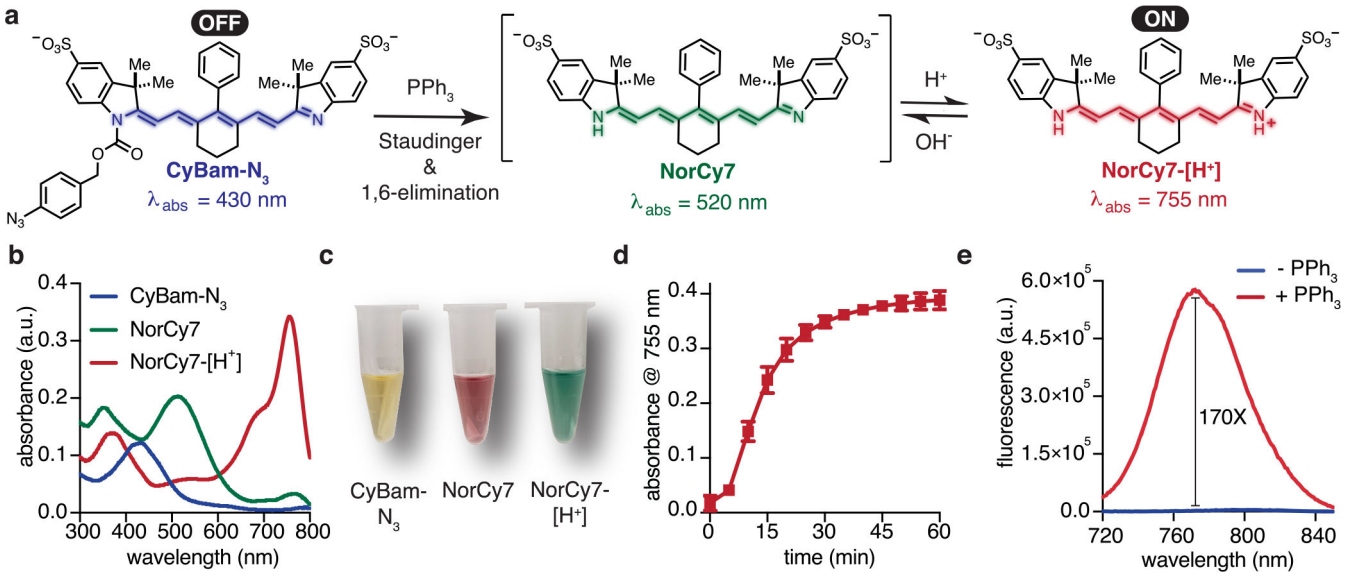

Figure 2.

(a) The turn-ON mechanism of **CyBam-N_3** is a two-step process requiring (i) cleavage of the carbamate linker and (ii) indolenine protonation. (b) Absorbance spectra and (c) images of 10 μM of solutions **CyBam-N_3** (blue) and **NorCy7** (green) in PBS, pH 7.4, and **NorCy7-[H^+]** (red) in acetate buffer, pH 5.2. (d) **CyBam-N_3** (10 μM; 1 equiv) and PPh_3 (100 μM; 10 equiv) in PBS:MeOH (1:1), pH 5.2, were monitored at 5 min intervals (n = 3). Complete conversion to **NorCy7-[H^+]** occurred within 60 min of PPh_3 addition. (e) Conversion of **CyBam-N_3** (10 μM) to **NorCy7-[H^+]** (100 μM PPh_3, pH 4.5) resulted in a 170× enhancement of the NIR fluorescent signal (ex. 710 nm).

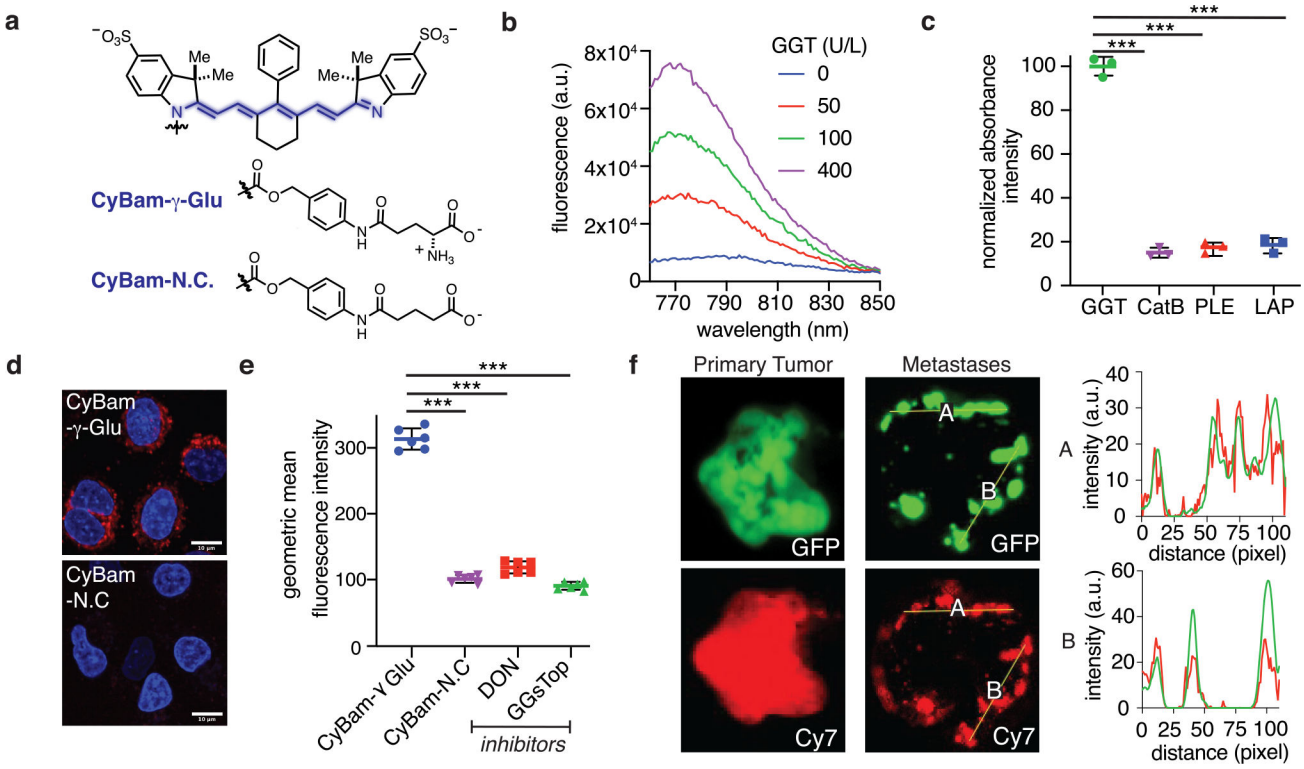

Figure 3.

(a) Structures of **CyBam-*γ*-Glu** and **CyBam-N.C.** (b) Increase in fluorescent intensity of **CyBam-*γ*-Glu** (20 *μ*M) after incubation with increasing concentration of GGT (0–400 U/L). (c) Activation of **CyBam-*γ*-Glu** after incubation with GGT (100 U/L), leucine aminopeptidase (LAP; 800 U/L), and pig-liver esterase (PLE; 800 U/L) at 37 °C for 30 min in PBS pH 7.4 followed by pH adjustment to pH 5.2. Cathepsin B (CatB; 2.5 *μ*g) was used in acetate buffer pH 5.2 for 30 min at 37 °C. (d) Confocal images of activation of **CyBam-*γ*-Glu** (20 *μ*M) and **CyBam-N.C.** (20 *μ*M) in SHIN-3 cells. The fluorescent signal from the probe and nucleus (Hoechst) is shown in red and blue, respectively. Images were taken using a 63× oil immersed lens (numerical aperture, N.A. 1.4). (e) Quantification of fluorescent signal after incubation of **CyBam-*γ*-Glu** (20 *μ*M) in the presence of GGT inhibitors (DON, GGsTop) and **CyBam-N.C.** in SHIN-3 cells using flow cytometry. The geometric mean fluorescent intensity (±SD) of the fluorescent signal in the cells is shown (*n* = 6 independent experiments). (f) *In vivo* imaging of the SHIN-3-ZsGreen metastatic tumor model at 3 h. Green and red pseudocolors are used to represent the signal from the GFP and Cy7 channels, respectively. Fluorescent line graph showing a correlation between the fluorescent signal from GFP and Cy7 channel across the metastatic tumor in two different regions (A and B). Data points are displayed as mean ± SD, and the *p*-values were evaluated by the Student's *t*-test (*** *p*-value ≤0.001).

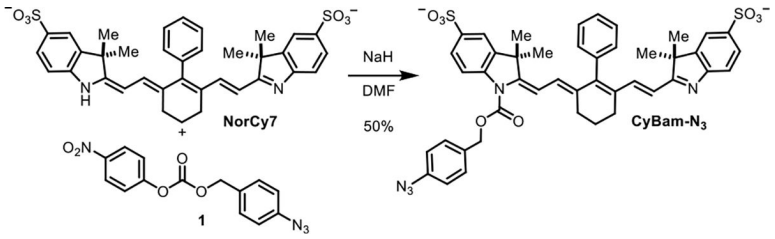

Scheme 1. Synthesis of CyBam-N_3